学　位　論　文

学位論文名

Mitochondrial-targeted antioxidants improve age-related collateral development with ischemia

（ミトコンドリア標的抗酸化薬は加齢に伴う虚血後の側副血行路発達不良を改善する　）

福島県立医科大学大学院医学研究科

循環血液病態情報学分野

循環器内科学講座

三浦　俊輔

概要:

【背景】加齢は虚血に伴う側副血行路の発達を阻害する重要な因子である。年齢に伴い増加する活性酸素もまた、側副血行路の発達障害に寄与すると考えられているが、その機序は未だ不明な点が多い。そこで、私たちはミトコンドリアが活性酸素の主な産生源であることに注目し、加齢に伴う下肢虚血後の側副血行路の発達障害において、ミトコンドリア由来活性酸素がどのように働いているのかを明らかにするため、加齢マウスを用い以下の実験を行った。
【方法・結果】加齢マウス（80 週令）を無作為に 2 群に分け、ミトコンドリア由来活性酸素除去薬である MitoTEMPO (180 μg/kg/日 28 日間)投与群、生理食塩水投与群とし、それぞれ浸透圧ポンプにて皮下投与した。また、同様に若年マウス (8 週令)に生理食塩水を皮下投与した。薬剤投与開始後、7 日目に片側の大腿動脈を結紮し、結紮直前、結紮直後、結紮後 1 日目、7 日目、14 日目、21 日目の下肢血流をレーザードップラー法にて評価した。虚血後下肢血流回復及び毛細血管密度は若年マウスと比較し、加齢マウスで低下しており、MitoTEMPO 投与加齢マウスにおいて改善を認めた。ミトコンドリア DNA 障害は加齢マウスの骨格筋において高度であり、MitoTEMPO の投与により抑制された。結紮後 2 日目の虚血骨格筋において MitoTEMPO 投与は加齢マウスの癌抑制遺伝子 p53 の発現を抑制し、アポトーシスに関与する Bax/Bcl2 発現比を低下させ、血管新生を促進する HIF-1α及び VEGF の発現を促進した。結紮後 21 日目の虚血骨格筋において MitoTEMPO 投与は peroxisome proliferator-activated receptor γ coactivator-1α (PGC-1α)及びその転写因子である estrogen-related receptor α (ERRα)、nuclear respiratory factor (NRF)-1 の発現を温存した。ヒラメ筋から抽出したミトコンドリアの呼吸調節率は非虚血及び虚血 2 日目においては若年マウス、加齢マウス、MitoTEMPO 投与加齢マウスの 3 群において有意差を認めなかったが、虚血 21 日目においては加齢マウスで有意に低下した。
【結論】本研究により加齢マウスに対するミトコンドリア由来活性酸素の除去が p53 の抑制、PGC-1α の保持と関連し、虚血後の側副血行路の回復を促すことが示唆された。

Abbreviations:

PGC-1α: peroxisome proliferator-activated receptor γ coactivator-1α

NRF: nuclear respiratory factor

ERRα: estrogen-related receptor α

ROS: reactive oxygen species

MitoTEMPO: 2-(2,2,6,6-Tetramethylpiperidin-1-oxyl-4-ylamino)-2-oxoethyl) triphenylphosphonium chloride monohydrate

H_2O_2: hydrogen peroxide

OCR: oxygen consumption rate

RCR: respiratory control ratio

FCCP: p-trifluoromethoxyphenylhydrazone

UPLC: ultra-performance liquid chromatography

POD: post-operative day

PAD: peripheral artery disease

CLI: critical limb ischemia

HEPES: 4-(2-hydroxyethyl)-1-piperazineethanesulfonic acid

EGTA: ethylene glycol-bis(2-aminoethylether)-N,N,N',N'-tetraacetic acid

MAS: mitochondrial assay solution

ADP: Adenosine 5'-diphosphate sodium

TBST: Tris-buffered saline Tween 20

VEGF: vascular endothelial growth factor

HIF-1α: hypoxia-inducible factor-1α

ETS: electron transport system

H&E: Hematoxylin and Eosin

1. Introduction

Senescence is an irreversible risk factor for most forms of cardiovascular and peripheral artery disease (PAD) (1, 2). Previous reports demonstrated aging-dependent impairment of collateral growth with critical limb ischemia (CLI) (3, 4). However, this mechanism remains complicated. Oxidative stress increase with age is one of the causes of collateral rarefaction (5). Age-dependent increases in oxidative stress occur through multiple mechanisms, including mitochondrial dysfunction. The mitochondria are major sources of reactive oxygen species (ROS), which are increased in aging animals (6). This increase in mitochondrial ROS is associated with the oxidation of the electron transport system (ETS) complex V, leading to decreased ATP production (7, 8) and increased DNA oxidative damage (7, 9). Moreover, in PAD patients, mitochondrial dysfunction and increased oxidative stress-induced damage have been reported (10, 11). Taken together, it seems that the resolution of mitochondrial ROS in aged mammals is attributed to collateral growth under ischemia through the recovery of mitochondria or other signaling pathways. In contrast, transient or low levels of ROS also act as mediators of angiogenesis through the HIF-VEGF/VEGFR2 signaling pathway and the VEGF-independent pathway, the latter of which involves the generation of lipid oxidation products (12). Therefore, we performed the present study to examine whether mitochondrial ROS scavenging improves collateral growth using acute hind limb ischemia in aged mice. In this study, collateral growth in old mice treated with MitoTEMPO (Fig. 1), which is speculated to reduce oxidative stress, was observed compared to young and old mice. We demonstrated the mechanism of angiogenesis with regard to p53 and the peroxisome proliferator-activated receptor γ coactivator-1α (PGC-1α) pathway as well as HIF-VEGF signaling. In addition, we elucidated the effect

of oxidative stress in aging with respect to mitochondrial DNA (mtDNA) and apoptosis.

2. Materials and Methods

Ethics statement

The investigations conformed to the Guide for the Care and Use of Laboratory Animals published by the US National Institutes of Health (NIH publication, 8th Edition, 2011). Our research protocol was approved by the Fukushima Medical University Animal Research Committee (permit number 27058), and all animal experiments were conducted in accordance with the guidelines of the Fukushima Medical University Animal Research Committee. All efforts were made to minimize animal suffering.

Animals

Young and old wild type C57BL/6 female mice［Young; 8 weeks (W), body weight (B.W.) 19.6±0.2 g, Old; 80 W, B.W. 28.4±0.3 g］were housed and bred in a room at 22 ± 3°C, with a relative humidity of 50 ± 10% and a 12-h light-dark cycle. The mice were given food and water *ad libitum*.

Animal experiments

The mice received a separate mini-pump for co-infusion of MitoTEMPO (Santa Cruz Biotechnology, Dallas, TX) or saline. The mice were anesthetized by tribromoethanol (200 mg/kg body weight, i.p.) and an osmotic mini-pump (ALZET micro-osmotic pump, model 1002, DURECT Co., Cupertino, CA) was subcutaneously implanted. MitoTEMPO (180 μg/kg/day) and saline for the old mice and saline for the young mice were continuously infused. From the previous study concerning to the hemodynamic

effect of MitoTEMPO, we determined 180 μg/kg/day of MitoTEMPO is a suitable dose (13). Unilateral hind limb ischemia was induced by ligation of the left femoral artery from its origin just below the inguinal ligament under tribromoethanol anesthesia (200 mg/kg body weight, i.p.) at day 7 after pump implantation (14). The sham operation was without femoral artery ligation but with skin incision in the right hind limb of ischemia-induced mice. The mice were sacrificed with isoflurane aspiration and a lethal dose of pentobarbital (60 mg/kg body weight i.p.) on postoperative day (POD) 2 or 21, and examinations were performed.

Measurement of hind limb perfusion

Scanning laser Doppler perfusion imaging (Moor Instruments, Wilmington, DE) was used to record the hind limb perfusion under 1.125% isoflurane/O_2 anesthesia (14). The ratio of ischemic-to normal laser Doppler blood flow was measured before ligation and on POD 0, 1, 7, 14 and 21. Average perfusion was recorded from the plantar to inguinal surface, which indexes overall limb blood flow, and is expressed as the ischemic/non-ischemic ratio for assessing the variables, including ambient light and temperature (14).

Mitochondrial isolation

Skeletal muscle mitochondria were isolated from the soleus of both ischemic and non-ischemic hind limbs based on previously reported protocols (15, 16). Briefly, each soleus was washed in mitochondria isolation buffer [MSHE: 70 mM sucrose, 210 mM mannitol, 5 mM HEPES, 1 mM EGTA, 0.5% fatty acid-free BSA (pH 7.2)], minced on ice and trypsinized for 2 min. Trypsinized muscles were homogenized using a Dounce

homogenizer in cold MSHE buffer. Homogenates were centrifuged at 800×g for 10 min. Supernatants were removed and centrifuged at 8000× g for 10 min. Pellets were washed three times in MSHE buffer without BSA and the protein was estimated using the Bradford protein assay (Bio-Rad, Hercules, CA). The mitochondrial pellet was resuspended at 10 μg/50 μl in mitochondria assay buffer [MAS: 70 mM sucrose, 220 mM Mannitol, 10 mM KH_2PO_4, 5 mM $MgCl_2$, 5 mM HEPES, 1 mM EGTA, 0.2% fatty acid-free BSA (pH 7.2)] for measurement of mitochondrial respiration and H_2O_2 concentration.

Mitochondrial H_2O_2 concentration measurement

The mitochondrial H_2O_2 concentration was measured using an Apollo 4000 Free Radical Analyzer equipped with a 100 μm H_2O_2 electrode (WPI Co., Sarasota, FL) as previously described (17). The measurements were performed on hot plate at 34℃ with a reaction volume of 500 μl. Each sample contained MAS buffer [70 mM sucrose, 220 mM Mannitol, 10 mM KH_2PO_4, 5 mM $MgCl_2$, 5 mM HEPES, 1 mM EGTA, 0.2% fatty acid-free BSA (pH 7.2)] and 50 μg of mitochondrial protein. Values were obtained at the point of a stable output signal and were converted to H_2O_2 concentration (μM/1 g of mitochondrial protein) using a predetermined H_2O_2 standard curve. To minimize errors, mitochondria were isolated on ice and the incubation-time was stabilized (17, 18).

Ultra-performance liquid chromatography (UPLC)

Dihydroethidium (DHE) can be oxidized by oxidants, leading to the formation of other fluorescent products such as 2-hydroxyethidium (EOH) and ethidium. EOH is mainly generated by a reaction with superoxide. We performed UPLC to separate and quantify

these products and to estimate superoxide levels in the gastrocnemius-soleus muscles as previously described (19). Ischemic and non-ischemic soleus 48 h after femoral artery ligation were immediately cut into 20 mg samples from the distal side and incubated with Krebs-HEPES buffer containing 50 μM DHE at 37°C for 30 min. The tissues were then washed with DHE in Krebs-HEPES buffer, placed in 300 μl of cold methanol and homogenized. After centrifugation (×8000 rpm, for 10 min), 200 μl of supernatant was exsiccated by nitrogen gas, dissolved in 100 μl of 0.2% formic acid, and filtered (0.22 μm). The filtrate was then analyzed by UPLC. Separation of 2-hydroxyethidium, ethidium and DHE was performed using a Waters AQUITY UPLC H-class system with an AQUITY BEH C18 column (particle size 1.7 μm, φ2.1x50 mm, Waters, Milford, MA) at 40℃.

Semi-quantitative PCR for mtDNA damage

mtDNA was isolated from 250 mg of hind limb skeletal muscle using a mtDNA extractor CT kit (Wako, Osaka, Japan). mtDNA damage was assayed by different length qPCR (20, 21). The principle of this assay is that lesions in mtDNA introduced by oxidative damage can block polymerase progression during PCR, reducing product abundance when compared to the undamaged DNA. We used a long 10-kb mtDNA target for analyzing oxidative damage, compared to a short 127-bp target as control for mtDNA copy number. Different length qPCR amplifications were conducted in a 50 μL volume containing 15 μg of mtDNA in 15 μl and 35 μl PCR mastermix [5 μg BSA, 200 μM dNTPs, 20 pmol forward and reverse primers, 0.1 mM Mg, 1 U/μl Ex Taq, 3.5 μl 10×EX Taq buffer (Takara-bio, Kusatsu, Japan) and 31.5 μl nuclease-free water]. The mouse large 10 kb mtDNA fragment primers were:

5’GCC AGC CTG ACC CAT AGC CAT AAT,

5’GAG AGA TTT TAT GGG TGT AAT GCG

Mouse small 127 bp mtDNA fragment primers were:

5’GCC AGC CTG ACC CAT AGC CAT AAT,

5’GCC GGC TGC GTA TTC TAC GTT A

The reactions were initiated with the hot start method. For long fragment PCR amplification, DNA was denatured initially at 75℃ for 2 min and 95℃ for 1 min, and then the reaction underwent 16 cycles of 94℃ for 15 sec, 64℃ for 12 mins, with a final extension of 72℃ for 10 minutes. For small fragment PCR amplification, DNA was denatured initially at 75℃ for 2 min and 95℃ for 15 sec, followed by 23 cycles of 94℃ for 30 sec, 64℃ for 45 sec, 72℃ for 45 sec, and then 72℃ for 10 min. PCR products were quantified by the PicoGreen ds DNA assay kit (Thermo Fisher scientific, Waltham, MA, USA) as per the manufacturer’s protocol. The amplification of the long product (A_L) was normalized to the short product (A_S) for each sample resulting in a relative amplification ratio. Using the ‘zero class’ of a Poisson equation, the lesion frequency per fragment at a particular dose was determined: $\lambda=\ln A_L/A_S$ (λ=the average lesion frequency) (22).

Measurement of mitochondrial respiration

Mitochondrial oxygen consumption was measured using the XF24 instrument (Seahorse Bioscience, North Billerica, MA) as reported previously (15). We plated 10 μg of skeletal muscle mitochondria in each well of the XF24 v7 plate in a volume of 50 μl containing MAS buffer with 10 mM succinate and 2 μM rotenone. After centrifugation (for 20 min at 2000 rpm), 450 μl of MAS containing succinate and rotenone was added

and incubated at 37℃ for 10 min. The plate with mitochondria was introduced into the XF machine and assayed using the protocol developed by Rodgers et al. (15). In this protocol, 50 μl of ADP (40 mM), 55 μl of oligomycin (25 μg/ml), 60 μl of carbonyl cyanide-p-trifluoromethoxy-phenylhydrazone (FCCP, 40 μM), and 65 μl of antimycin A (40 μM) were injected into each sample in sequence. Therefore, the final concentrations were: ADP 4 mM, oligomycin 2.5 μM, FCCP 4 mM and antimycin A 4 μM. Oxygen consumption rates (pmols oxygen per minute) were monitored in real time and we could determine basal respiration (state 2 respiration), phosphorylating respiration in the presence of ADP (state 3 respiration), resting respiration (state 4 respiration), maximal uncoupling respiration in the presence of FCCP (state 3u respiration) and electron transport chain-unrelated respiration in the presence of complex III inhibitor antimycin A. The respiratory control ratio (RCR) was determined by dividing the rate of state 3 respiration by state 4 respiration.

Immunohistochemistry

Bilateral gastrocnemius-soleus muscles were dissected and snap-frozen in a bath of liquid nitrogen on postoperative day 21. Muscles were sectioned on a cryostat to a thickness of 7 μm and fixed in 100% methanol and H_2O_2. Immunohistostaining was performed with rabbit anti-mouse CD31 antibody (Santa Cruz Biotechnology) and an anti-rabbit Ig horseradish peroxidase detection kit (Nichirei biosciences, Chuo, Japan). The capillary count was performed under light microscopy (magnification ×200). The number of capillaries per muscle fiber was measured in 5 randomly chosen fields from 3 different sections in each tissue block (23). For demonstrate representative morphology of ischemic muscles, sections were stained with Hematoxylin and Eosin (H&E).

Western blotting

Frozen gastrocnemius-soleus muscles were pulverized in liquid nitrogen and suspended in lysis buffer with protease inhibitor. After quantifying the protein concentrations using the Bradford protein assay (Bio-Rad), equal amounts of protein (20 μg/sample) were analyzed by 10 or 15% SDS-PAGE gels depending on the molecular weight. The gels were transferred onto nitrocellulose membranes. Membranes were blocked in Tris-buffered saline Tween 20 (TBST) containing 5% BSA and immunoblotted using the following primary antibodies: anti-p53 (PAb122) antibody (Enzo Life Science, Inc, Farmingdale, NY, 1:1500), anti-PGC1 alpha (ab54481) antibody (Abcam, Cambridge, UK, 1:1500), anti-HIF-1α(#14179) antibody (Cell Signaling, Danvers, MA, 1:1000), anti-Bax (2772) antibody (Cell Signaling, 1:1000), anti-Bcl-2 (2876) antibody (Cell Signaling, 1:1000), anti-VEGF (sc-507) antibody (Santa Cruz Biotechnology, 1:1000), anti-β-Actin (sc-47778) antibody (Santa Cruz Biotechnology, 1:10000), anti-ERR alpha (EPR46Y)) antibody (Novus Biologicals, Littleton, CO, 1:1000), and anti-NRF1 (200-401-869) antibody (Rockland, Limerick, PA, 1:1000). Membranes were then washed in TBST and incubated with the appropriate anti-mouse or anti-rabbit horse radish peroxidase-linked secondary antibody (Santa Cruz Biotechnology, 1:10000). Antibody-bound protein was visualized using the enhanced chemiluminescent method. The relative intensities of the protein bands were quantified using NIH Image J, version (1.48) (Scion Image, NIH). Data were normalized to β-actin and are expressed as a fold change to the non-ischemic skeletal muscle of young mice in the same period for each analysis.

Statistical analysis

Values are expressed as the means±S.E.M. One-way ANOVA with Tukey's post hoc test was used for comparisons among multiple groups. A *P* value less than 0.05 was considered to be statistically significant. All statistical analyses were performed using SPSS software program (ver.23.0, IBM, Armonk, NY)

3. Results

The levels of mitochondrial H_2O_2 and superoxide in skeletal muscle

Because the increase in mitochondrial ROS is assumed to be a major factor in the decline of collateral growth with ischemia, we initially measured the level of mitochondrial H_2O_2 in the non-ischemic and ischemic skeletal muscles of young, old and MitoTEMPO-treated old mice in POD 2. There was no significant difference among the three groups in non-ischemic skeletal muscles. Under ischemic condition, the level of mitochondrial H_2O_2 was elevated in only the old mice compared to non-ischemic one. Moreover, the level of mitochondrial H_2O_2 was higher in the old mice than young mice under ischemic conditions. MitoTEMPO treatment decreased the level of mitochondrial H_2O_2 to the level of young mice (Fig. 2A). Since mitochondria are the major source of ROS in aging tissues (24, 25), mitochondrial-targeted antioxidants may contribute to decreased ROS in tissues. To determine whether MitoTEMPO could reduce ROS in tissues, we measured the levels of superoxide in the hind limb by the UPLC method. The levels of superoxide in non-ischemic hind limb tissue did not differ among the three groups. The level of superoxide was elevated in the ischemic hind limb of old mice compared to non-ischemic mice (P=0.029). In young and MitoTEMPO-treated old mice, the levels of superoxide were not increased by

ischemia. The levels of superoxide in tissue extracts under ischemia were higher in old mice than in young mice, and those were reduced by MitoTEMPO treatment. (44948.1±7266.3 vs. 17008.5±3133.1 and 26004.0±2234.3 mVs/μmol, respectively, n=10, $P<0.05$, Fig. 2B)

Collateral flow recovery

We examined the effect of MitoTEMPO on age-related impairment of collateral growth using laser Doppler perfusion imaging. The collateral flow recovery was more impaired in the ischemic hind limb of old mice than in those of young mice. MitoTEMPO treatment improved the collateral flow recovery (Fig. 3A and B). The improvement of collateral flow recovery was reflected by an increase in capillary density as determined by CD 31 staining of the gastrocnemius-soleus muscle (Fig. 3C and D). These data suggest that mitochondrial ROS scavenging recovers the age-related impairment of collateral growth.

mtDNA damage

mtDNA is highly susceptible to oxidative stress because of the absence of protective histones, leading to more vulnerable nuclear DNA. Mitochondrial ROS increase with age and are associated with oxidative mitochondrial DNA damage and endothelial/vascular dysfunction (26). To examine whether MitoTEMPO treatment prevented the mtDNA damage induced by aging and ischemia, we performed different length qPCR for the mtDNA of both ischemic and non-ischemic skeletal muscles. mtDNA damage was increased in old mice compared to young mice and

MitoTEMPO-treated old mice (0.45±0.02 vs. 0.10±0.08 and 0.15±0.03 lesions/10 kb, n=10, $P<0.05$, respectively) after ischemia but not in non-ischemic skeletal muscles on POD 2 (Fig. 4). These results suggest that mtDNA damage induced by ischemia increases with senescence, but is suppressed by mitochondrial ROS scavenging.

Respiratory profile of mitochondria in skeletal muscle

Although a few reports have described age-related impairment of mitochondrial respiration in skeletal muscle (27), most studies find no age-related changes in mitochondrial respiration (28, 29). However, how ischemia alters the mitochondrial respiration profile in aging skeletal muscle is not fully understood. Moreover, the effect of mitochondrial ROS scavenging for ischemic skeletal muscle is unclear. Thus, we examined the change in the mitochondrial respiration profile of ischemic skeletal muscles using a XF24 flux analyzer. We chose the soleus to minimize errors because mitochondrial respiratory function is muscle type specific and the soleus is primarily composed of slow twitch fibers (30). In non-ischemic skeletal muscles, mitochondrial respiration via complex II, including state 2, state 3, state 4, state 3u and in response to antimycin A, did not differ among young, old and Mito-TEMPO-treated old mice (Fig. 5B). In ischemic skeletal muscles of POD 2, the respiration rate of each state was higher in young mice than old mice (Fig. 5C). This analysis did not reveal a significant effect of MitoTEMPO treatment because the duration of treatment of MitoTEMPO may have been too short, which necessitates further study. In ischemic skeletal muscles at POD 21, the respiration rate of each state was higher in young mice than in old mice. Furthermore, MitoTEMPO treatment significantly preserved mitochondrial respiration

compared to no treatment (Fig. 5D). These data suggest that MitoTEMPO treatment in old mice could preserve mitochondrial respiration under ischemia to a similar level as that of young mice. The respiratory control ratio (RCR, state 3/state 4) is an index of coupling for diagnosis of ETS defects, indicating the efficiency of ATP production in the presence of ADP. In ischemic skeletal muscles at POD 21, the mitochondria of old mice displayed a lower RCR value than those of young mice, and MitoTEMPO treatment elevated RCR value to the level as young mice (Fig. 5E). The RCR value of both non-ischemic and ischemic skeletal muscles at POD 2 revealed no differences among the three groups (Fig. 5E). These data suggested that MitoTEMPO treatment for old mice may have contributed to the preservation of ATP production through ETS in chronically ischemic skeletal muscle.

The protein expression of hypoxia-inducible factor-1α (HIF-1α) and VEGF

HIF-1α and VEGF levels are known to decrease with aging (31, 32). According to previous reports, excessive oxidative stress can impair VEGF-induced angiogenesis in endothelial cells (33). To examine the proangiogenic effect of mitochondrial ROS scavenging, we examined the protein expression of HIF-1α and VEGF by western blot analysis. In non-ischemic skeletal muscles, the protein expression levels of HIF-1α (Fig. 6A) and VEGF (Fig. 6B) did not differ among young, old and MitoTEMPO-treated old mice. However, at POD 2 after ischemia, HIF-1α (Fig. 6A) and VEGF expression (Fig. 6B) were significantly induced in young mice. The elevation of HIF-1α and VEGF expression were suppressed in old mice, which were recovered by MitoTEMPO treatment. These data suggest that mitochondrial ROS scavenging is associated with elevated HIF-1α and VEGF expression levels in old skeletal muscle. On POD 21 after

ischemia, the expression levels of HIF-1α and VEGF in old mice were lower than those of young mice (Fig. 6C and D). In ischemic conditions, the expression level of HIF-1α in old mice was not different from that in young mice. In addition, the magnitude of HIF-1α was smaller than that in POD 2 in the same conditions. Therefore, we propose that the contribution of HIF-1α to angiogenesis is rare in the late phase of ischemia.

The protein expression of p53

The tumor suppressor p53 responds to hypoxia and is stabilized during severe hypoxia (34). In severe hypoxia, p53 competes with HIF-1α to binding to p300, leading to HIF-1α downregulation (35). Moreover, according to previous reports, oxidative mitochondrial damage causes p53 activation (36). Taking into account our finding that decreasing mitochondrial ROS led to HIF-1α upregulation, we assumed that MitoTEMPO treatment could downregulate p53 expression. Thus, we examined whether MitoTEMPO treatment can attenuate the p53 expression in ischemic aged skeletal muscle. In non-ischemic skeletal muscle, the expression of p53 was higher in old mice than in young mice. MitoTEMPO treatment failed to reduce p53 in old mice. The p53 expression in ischemic muscle at POD 2 in old mice was markedly higher compared to young mice, which was attenuated by MitoTEMPO treatment (Fig. 7). These findings suggest that mitochondrial ROS scavenging in aged skeletal muscle attenuates p53 upregulation under ischemia. This mechanism may contribute to the upregulation of HIF-1α under ischemia.

The protein expression of PGC-1α, ERRα and NRF-1

The transcriptional coactivators of PGC-1α have been identified as crucial regulators of

mitochondrial biogenesis and function (37, 38). In addition, PGC-1α has been shown to mediate a HIF-1-independent pathway of angiogenesis in response to hypoxia (39). Thus, we examined the effect of mitochondrial ROS scavenging for PGC-1α and its transcriptional factors, estrogen-related receptor α (ERRα) and nuclear respiratory factor (NRF)-1 expression under ischemia. In non-ischemic skeletal muscle, the expression of PGC-1α, ERRα and NRF-1 did not differ among three groups (Fig. 8A-D). We also could not find a significant difference between these factors in ischemic skeletal muscle at POD 2 (Fig. 8A-D). Meanwhile, in ischemic skeletal muscles at POD 21, the expression of PGC-1α, NRF-1 and ERRα were lower in old mice than in young mice. MitoTEMPO treatment recovered the expression of PGC-1α, NRF-1 and ERRα to similar levels as young mice (Fig. 8E-H). We found that mitochondrial ROS scavenging preserved the expressions of PGC-1α and its transcriptional factors in aged skeletal muscles during prolonged ischemia, indicating the involvement of angiogenesis in the chronic phase of ischemia. This finding also supports reduced mitochondrial respiration in ischemic aged skeletal muscle at POD 21.

The expression of apoptotic factors

Apoptosis is a well-known anti-angiogenetic mechanism. According to previous reports, p53 mediates apoptosis by activating proapoptotic genes (Bak, Bax) and repressing antiapoptotic Bcl2 family genes (40, 41). Thus, we tested whether resolution of mitochondrial ROS could prevent ischemia-induced apoptosis. Western blot analysis revealed the elevated expression of Bax and the Bax/Bcl2 ratio in old mice compared to young mice (Fig. 9A-D). MitoTEMPO treatment decreased the expression of Bax and the Bax/Bcl2 ratio to the level of young mice (Fig. 9A-D). Overall, these data suggest

that attenuating mitochondrial ROS recovered the ischemia-induced apoptotic changes in aged skeletal muscles. The ratio of the weight of the ischemic hind limb and the gastrocnemius-soleus muscle (POD 21) per non-ischemic muscles were reduced in old mice compared to those in young and MitoTEMPO-treated old mice (Table), which may reflect the consequences of muscular apoptosis.

4. Discussion

Senescence is related to most forms of cardiovascular disease (1, 2). Our results demonstrate that oxidative stress plays a crucial role in the age-associated impairment of collateral growth, shedding light on the role of mitochondrial ROS in aging skeletal muscle. Moreover, we showed that mitochondrial ROS-targeted therapy for aging skeletal muscle attenuates mitochondrial DNA damage, mitochondrial dysfunction and apoptosis under ischemia, thus contributing to angiogenesis.

Our main findings are that administration of a mitochondria-targeted antioxidant, MitoTEMPO, leads the downregulation of p53 and the preservation of PGC-1α, which may be associated with angiogenesis, apoptosis and mitochondrial function. The tumor suppressor p53 is upregulated in response to cellular stress, including DNA damage, oxidative stress and hypoxia (42). Activated p53 interferes with hypoxia-sensing systems and degrades HIF-1α, leading to impaired VEGF expression (43). In addition, p53 is the pivotal factor that induces apoptosis by recognizing external stimuli (40, 41, 44). For example, in an ischemia/reperfusion model of aged rats, inhibition of p53 by pifithrin-α has a protective effect, thereby attenuating p53/Bax-mediated myocyte apoptosis during the early stages of ischemia (45). In our study, p53 was upregulated by

aging and ischemic stimuli, which seemed to lead to apoptosis and inhibit angiogenesis through the HIF-1/VEGF axis. In contrast, MitoTEMPO treatment could effectively downregulate p53 expression. Taking into account the fact that ROS itself activates p53, decreasing ROS and DNA damage by mitochondrial-targeted antioxidants is likely the main reason for the downregulation of p53. Although p53 is thought to act as an anti-angiogenetic factor in contrast to VEGF, ischemic stimuli elevated p53 expression not only in old mice but also in young and old mice treated with MitoTEMPO. According to previous reports, p53 represses VEGF expression under continued hypoxic conditions. However, it can also positively regulate VEGF expression during the initial phase of hypoxia by binding to conserved sites in the VEGF promoter (46). Thus, the elevation of p53 is crucial in the early phases of ischemia induction, and our results seem to be compatible with this previous report. PGC-1α also dramatically induces angiogenesis through a HIF-1-independent pathway (39). PGC-1α binds to its transcriptional genes such as ERRα and NRFs, allowing for the induction of angiogenic genes and mitochondrial genes (47). In our study, MitoTEMPO treatment could not elevate the level of PGC-1α expression in ischemic skeletal muscle (POD 2). Therefore, it is likely that mitochondrial ROS scavenging does not affect angiogenesis in the early phase of ischemia. However, in the late phase (POD 21), the expression of PGC-1α and its transcriptional factor were preserved by MitoTEMPO treatment. Several reports demonstrated that PGC-1 is induced by increased physical activity or exercise training, leading to angiogenesis and mitochondrial biogenesis (48, 49). In our study, the weight of the ischemic hind limb in old mice was reduced, seemingly as a result of the apoptosis of skeletal muscle (Table). This finding is likely related to muscular atrophy and low physical activity, which may be attributed to low PGC-1α expression and an

altered mitochondrial respiratory profile in skeletal muscle (Fig. 10). We emphasize that mitochondrial ROS scavenging works effectively to preserve PGC-1α expression through inhibition of apoptosis or preservation of physical activity.

It is controversial whether mitochondrial respiration decreases with senescence. Recently, some studies demonstrated that mitochondrial respiration or electron transport chain (ETC) activity show strong dependency on the physical activity level, independent of aging (50, 51). Our study revealed a lower mitochondrial respiration and RCR value in old mouse skeletal muscle under chronic ischemic conditions than in young and Mito-TEMPO-treated mice. This result also seems to be associated with low PGC-1α expression due to a low physical activity level because PGC-1α works as a master regulator of mitochondrial biogenesis. We cannot confirm whether this age-related alteration of the mitochondrial profile is a cause or consequence of impaired collateral growth under ischemia. However, taking into account the fact that the ATP produced in mitochondria is critical for maintaining the energy status of the cell, an altered mitochondrial profile may possibly attribute to collateral development.

There are a few limitations in this study. First, the current work did not show eNOS activity. eNOS is crucial for VEGF-triggered angiogenesis because NO stimulates VEGF, and eNOS also acts as an essential effector of downstream VEGF signaling for angiogenesis (52, 53). However, our previous study revealed that MitoTEMPO treatment recovered eNOS function and activity in the ischemic muscle of old mice (13). Thus, preservation of eNOS activity by MitoTEMPO may contribute to improvements in age-related collateral development. Second, we did not demonstrate whether the effect of MitoTEMPO is dose-dependent. It has been reported that a low level of ROS is essential for angiogenesis through HIF-VEGF pathway signaling (12). In our study,

MitoTEMPO treatment did not suppress angiogenesis because MitoTEMPO treatment did not decrease mitochondrial H_2O_2 and superoxide in ischemic skeletal muscle to the level of non-ischemic mice. However, in the case of higher dose of MitoTEMPO, angiogenesis under ischemia may be attenuated due to an insufficient amount of ROS.

5. Conclusion

Our findings suggest that mitochondrial ROS scavenging contributes to the attenuation of age-dependent mitDNA damage and excessive ROS elevation after ischemia. We also demonstrated that mitochondrial ROS induced by ischemia impairs collateral development, and mitochondrial ROS scavenging improves collateral growth related to downregulation of p53, upregulation of HIF-1α and VEGF in the early phase of ischemia, and preservation of PGC-1α, NRF-1, and ERRα in the late phase of ischemia(Fig. 10). Overall, treatment of mitochondria-targeted antioxidants can be an effective therapy to improve quality of life and outcomes in CLI patients.

6. Acknowledgements

We acknowledge the care of mice by Emiko Kaneda, Tomiko Miura and the animal institute of Fukushima Medical University.

7. Disclosures

No conflicts of interest, financial or otherwise, are declared by the authors.

8. References

1. Cooper LT, Cooke JP, Dzau VJ. The vasculopathy of aging. J Gerontol. 1994; 49:

B191–B196.

2. Lloyd-Jone D, Adams RJ, Brown TM. Heart disease and stroke statistics-2010 update: a report from the American Heart Association. Circulation. 2010; 121: e46–e215.
3. Rivard A, Fabre JE, Silver M, Chen D, Murohara T, Kearney M, Magner M, Asahara T, Isner JM. Age-dependent impairment of angiogenesis. Circulation. 1999; 99: 111-120.
4. Bosch-Marce M, Okuyama H, Wesley JB, Sarkar K, Kimura H, Liu YV, Zhang H, Strazza M, Rey S, Savino L, Zhou YF, McDonald KR, Na Y, Vandiver S, Rabi A, Shaked Y, Kerbel R, Lavallee T, Semenza GL. Effects of aging and hypoxia-inducible factor-1 activity on angiogenic cell mobilization and recovery of perfusion after limb ischemia. Circ Res. 2007; 101: 1310-1318.
5. Miller SJ, Coppinger BJ, Zhou X, Unthank JL. Antioxidants reverse age-related collateral growth impairment. J Vasc Res. 2010; 47: 108-114.
6. Sohal RS, Sohal BH. Hydrogen peroxide release by mitochondria increases during aging. Mech Ageing Dev. 1991; 57: 187-202.
7. Mansouri A, Muller FL, Liu Y, Ng R, Faulkner J, Hamilton M, Richardson A, Huang TT, Epstein CJ, VanRemmen H. Alterations in mitochondrial function, hydrogen peroxide release and oxidative damage in mouse hind-limb skeletal muscle during aging. Mech Ageing Dev. 2006; 127: 298-306.
8. Yarian CS, Rebrin I, Sohal RS. Aconitase and ATP synthase are targets of malondialdehyde modification and undergo an age-related decrease in activity in mouse heart mitochondria. Biochem Biophys Res Commun. 2005; 330: 151-156.
9. Chabi B, Ljubicic V, Menzies KJ, Huang JH, Saleem A, Hood DA. Mitochondrial

function and apoptotic susceptibility in aging skeletal muscle. Aging Cell. 2008; 7: 2-12.

10. Brass EP, Wang H, Hiatt WR. Multiple skeletal muscle mitochondrial DNA deletions in patients with unilateral peripheral arterial disease. Vasc Med. 2000; 5: 225-230.
11. Thompson JR, Swanson SA, Haynatzki G, Koutakis P, Johanning JM, Reppert PR, Papoutsi E, Miserlis D, Zhu Z, Casale GP, Pipinos II. Protein concentration and mitochondrial content in the gastrocnemius predicts mortality rates in patients with peripheral arterial disease. Ann Surg. 2015; 261: 605-610.
12. Kim YW, Byzova TV. Oxidative stress in angiogenesis and vascular disease. Blood. 2014; 123: 625-631.
13. Owada T, Yamauchi H, Saitoh S, Miura S, Machii H, Takeishi Y. Resolution of mitochondrial oxidative stress improves aged-cardiovascular performance. Coron Artery Dis. 2017; 28: 33-43.
14. Yamauchi H, Miura S, Owada T, Saitoh S, Machii H, Yamada S, Ishigami A, Takeishi Y. Senescence marker protein-30 deficiency impairs angiogenesis under ischemia. Free Radical Biol Med. 2016; 94: 66-73.
15. Rogers GW, Brand MD, Petrosyan S, Ashok D, Elorza AA, Ferrick DA, Murphy AN. High throughput microplate respiratory measurements using minimal quantities of isolated mitochondria. PLoS One. 2011; 6: e21746.
16. Frezza C, Cipolat S, Scorrano L. Organelle isolation: functional mitochondria from mouse liver, muscle and cultured fibroblasts. Nat Protoc. 2007; 2(2): 287-95.
17. Machii H, Saitoh SI, Kaneshiro T, Takeishi Y. Aging impairs myocardium-induced dilation in coronary arterioles: Role of hydrogen peroxide and angiotensin. Mech

Aging Develop. 2010; 131: 710-717.

18. Saitoh SI, Zhang C, Tune JD, Potter B, Kiyooka T, Rogers PA, Knudson JD, Dick GM, Swafford A, Chilian WM. Hydrogen peroxide: a feed-forward dilator that couples myocardial metabolism to coronary blood flow. Arterioscler Thromb Vasc Biol. 2006; 26: 2614-2621.
19. Shimizu T, Suzuki S, Sato A, Nakamura Y, Ikeda K, Saitoh SI, Misaka S, Shishido T, Kubota I, Takeishi Y. Cardio-protective effects of pentraxin 3 produced from bone marrow-derived cells against ischemia/reperfusion injury. J Mol Cell Cardiol. 2015; 89: 306-313.
20. Rudi K, Hagen I, Johnsrud BC, Skjefstad G, Tryland I. Different length (DL) qPCR for quantification of cell killing by UV-induced DNA Damage. Int J Environ Res Public Health. 2010; 7: 3376-3381.
21. Mercer JR, Cheng KK, Figg N, Gorenne I, Mahmoudi M, Griffin J, Vidal-Puig A, Murphy MP, Bennett M. DNA damage links mitochondrial dysfunction to atherosclerosis and the metabolic syndrome. Circ Res. 2010; 107: 1021-1031.
22. Furda A, Santos JH, Meyer JN, Van Houten B. Quantitative PCR-based measurement of nuclear and mitochondrial DNA damage and repair in mammalian cells. Methods Mol Biol. 2014; 1105: 419-437.
23. Cheng XW, Kazuya M, Nakamura K, Maeda K, Tsuzuki M, Kim W, Sasaki T, Liu Z, Inoue N, Kondo T, Jin H, Numaguchi Y, Okumura K, Yokota M, Iguchi A, Murohara T. Mechanisms underlying the impairment of ischemia-induced neovascularization in matrix metalloproteinase 2-deficient mice. Circ Res. 2007; 100: 904-913.
24. Cadenas E, Davies KJ. Mitochondrial free radical generation, oxidative stress, and

aging. Free Radic Biol Med. 2000; 29: 222-230.

25. Lenaz G, Bovina C, D'Aurelio M, Fato R, Formiggini G, Genova ML, Giuliano G, Merlo Pich M, Paolucci U, Parenti Castelli G, Ventura B. Role of mitochondria in oxidative stress and aging. Ann N Y Acad Sci. 2002; 959: 199-213.
26. Wenzel P, Schuhmacher S, Kienhöfer J, Müller J, Hortmann M, Oelze M, Schulz E, Treiber N, Kawamoto T, Scharffetter-Kochanek K, Münzel T, Bürkle A, Bachschmid MM, Daiber A. Manganese superoxide dismutase and aldehyde dehydrogenase deficiency increase mitochondrial oxidative stress and aggravate age-dependent vascular dysfunction. Cardiovasc Res. 2008; 80: 280-289.
27. Siegel MP, Kruse SE, Percival JM, Goh J, White CC, Hopkins HC, Kavanagh TJ, Szeto HH, Rabinovitch PS, Marcinek DJ. Mitochondrial-targeted peptide rapidly improves mitochondrial energetics and skeletal muscle performance in aged mice. Aging Cell. 2013; 12: 763-771.
28. Hütter E, Skovbro M, Lener B, Prats C, Rabøl R, Dela F, Jansen-Dürr P. Oxidative stress and mitochondrial impairment can be separated from lipofuscin accumulation in aged human skeletal muscle. Aging Cell. 2007; 6: 245-256.
29. Rasmussen UF, Krustrup P, Kjaer M, Rasmussen HN. Experimental evidence against the mitochondrial theory of aging. A study of isolated human skeletal muscle mitochondria. Exp Gerontol. 2003; 38: 877-886.
30. Kruse SE, Karunadharma PP, Basisty N, Johnson R, Beyer RP, MacCoss MJ, Rabinovitch PS, Marcinek DJ. Age modifies respiratory complex I and protein homeostasis in a muscle type-specific manner. Aging Cell. 2016; 15: 89-99.
31. Bosch-Marce M, Okuyama H, Wesley J, Sarkar K, Kimura H, Liu YV, Zhang H, Strazza M, Rey S, Savino L, Zhou Y, McDonald KR, Na Y, Vandiver S, Rabi A,

Shaked Y, Kerbel R, Lavallee T, Semenza GL. Effects of aging and hypoxia-inducible factor-1 activity on angiogenic cell mobilization and recovery of perfusion after limb ischemia. Circ Res. 2007; 101: 1310-1318.

32. Wagatsuma A. Effect of aging on expression of angiogenesis-related factors in mouse skeletal muscle. Exp Gerontol. 2006; 41: 49-54.
33. Lefèvre J, Michaud SE, Haddad P, Dussault S, Ménard C, Groleau J, Turgeon J, Rivard A. Moderate consumption of red wine (cabernet sauvignon) improves ischemia-induced neovascularization in ApoE-deficient mice: effect on endothelial progenitor cells and nitric oxide. FASEB J. 2007; 21: 3845-3852.
34. Hammond EM, Denko NC, Dorie MJ, Abraham RT, Giaccia AJ. Hypoxia links ATR and p53 through replication arrest. Mol Cell Biol. 2002; 22: 1834-1843.
35. Zhou CH, Zhang XP, Liu F, Wang W. Modeling the interplay between the HIF-1 and p53 pathways in hypoxia. Sci Rep. 2015; 5: 13834.
36. Villeneuve C, Guilbeau-Frugier C, Sicard P, Lairez O, Ordener C, Duparc T, De Paulis D, Couderc B, Spreux-Varoquaux O, Tortosa F, Garnier A, Knauf C, Valet P, Borchi E, Nediani C, Gharib A, Ovize M, Delisle MB, Parini A, Mialet-Perez J. p53-PGC-1α pathway mediates oxidative mitochondrial damage and cardiomyocyte necrosis induced by Monoamine Oxidase-A upregulation: Role in chronic left ventricular dysfunction in mice. Antioxid Redox Signal. 2013; 18: 5-18.
37. Handschin C, Spiegelman BM. Peroxisome proliferator-activated receptor gamma coactivator 1 coactivators, energy homeostasis, and metabolism. Endocr Rev. 2006; 27: 728-735.
38. Mirebeau-Prunier D, Le Pennec S, Jacques C, Gueguen N, Poirier J, Malthiery Y, Savagner F. Estrogen-related receptor alpha and PGC-1-related coactivator

constitute a novel complex mediating the biogenesis of functional mitochondria. FEBS J. 2010; 277: 713-725.

39. Arany Z, Foo SY, Ma Y, Ruas JL, Bommi-Reddy A, Girnun G, Cooper M, Laznik D, Chinsomboon J, Rangwala SM, Baek KH, Rosenzweig A, Spiegelman BM. HIF-independent regulation of VEGF and angiogenesis by the transcriptional coactivator PGC-1α. Nature. 2008; 451: 1008-1012.
40. Marchenko ND, Moll UM. Mitochondrial death functions of p53. Mol Cell Oncol. 2014; 1: e955995.
41. Chipuk JE, Kuwana T, Bouchier-Hayer L, Droin NM, Newmeyer DD, Schuler M, Green DR. Direct activation of Bax by p53 mediates mitochondrial membrane permeabilization and apoptosis. Science. 2004; 303: 1010-1014.
42. Vousden KH, Prives C. Blinded by the light: the growing complexity of p53. Cell. 2009; 137: 413-431.
43. Sano M, Minamino T, Toko H, Miyauchi H, Orimo M, Qin Y, Akazawa H, Tateno K, Kayama Y, Harada M, Shimizu I, Asahara T, Hamada H, Tomita S, Molkentin JD, Zou Y, Komuro I. p53-induced inhibition of Hif-1 causes cardiac dysfunction during pressure overload. Nature. 2007; 446: 444-448.
44. Maritsi D, Stagikas D, Charalabopoulos K, Batistatou A. What's new in p53? Hippokratia. 2006; 10: 116-119.
45. Liu P, Xu B, Cavalieri TA and Hock CE. Pifithrin-alpha attenuates p53-mediated apoptosis and improves cardiac function in response to myocardial ischemia/reperfusion in aged rats. Shock. 2006; 26: 608-614.
46. Farhang Ghahremani M, Goossens S, Haigh JJ. The p53 family and VEGF regulation: "It's complicated". Cell Cycle. 2013; 12: 1331-1332.

47. Thom R, Rowe GC, Jang C, Safdar A, Arany Z. Hypoxic induction of vascular endothelial growth factor (VEGF) and angiogenesis in muscle by truncated peroxisome proliferator-activated receptor γ coactivator (PGC)-1α. J Biol Chem. 2014; 289: 8810-8817.
48. Chinsomboon J, Ruas J, Gupta R, Thom R, Shoag J, Rowe G, Sawada N, Raghuram S, Arany Z. The transcriptional coactivator PGC-1alpha mediates exercise-induced angiogenesis in skeletal muscle. Proc Natl Acad Sci U S A. 2009; 106: 21401-21406.
49. Geng T, Li P, Okutsu M, Yin X, Kwek J, Zhang M, Yan Z. PGC-1alpha plays a functional role in exercise-induced mitochondrial biogenesis and angiogenesis but not fiber-type transformation in mouse skeletal muscle. Am J Physiol Cell Physiol. 2010; 298: C572-579.
50. Figueiredo PA, Powers SK, Ferreire RM, Amado F, Appell HJ, Duarte JA. Impact of lifelong sedentary behavior on mitochondrial function of mice skeletal muscle. J Gerontol A Biol Sci Med Sci. 2009; 64: 927-939.
51. Alves RM, Vitorino R, Figueiredo P, Duarte JA, Ferreira R, Amado F. Lifelong physical activity modulation of the skeletal muscle mitochondria proteome in mice. J Gerontol A Biol Sci Med Sci. 2010; 65: 832-842.
52. Murohara T, Asahara T, Silver M, Bauters C, Masuda H, Kalka C, Kearney M, Chen D, Symes JF, Fishman MC, Huang PL, Isner JM. Nitric oxide synthase modulates angiogenesis in response to tissue ischemia. J Clin Invest. 1998; 101: 2567-2578.
53. Couffinhal T, Silver M, Zheng LP, Kearney M, Witzenbichler B, Isner JM. Mouse model of angiogenesis. Am J Pathol. 1998; 152: 1667-1679.

9. Figures and Figure legends

Fig. 1. Pharmacological profile of MitoTEMPO

MitoTEMPO

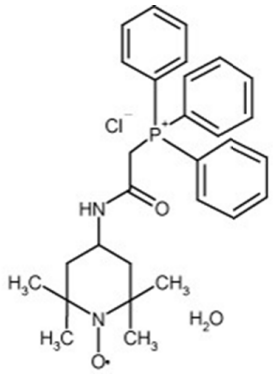

Synonium: (2-(2,2,6,6-Tetramethylpiperidin-1-oxyl-4-ylamino)-2-oxoethyl) triphenylphosphonium chloride monohydrate

Application: A mitochondria-targeted antioxidant with superoxide and alkyl radical scavenging properties

Molecular Weight: 528.04

Molecular Formula: $C_{29}H_{35}N_2O_2ClP\ H_2O$

MitoTEMPO consists of free radical scavenger, TEMPO (2, 2, 6, 6-tetramethylpiperidine 1-oxyl) and lipophilic triphenylphosphonium cation. Lipophilic triphenylphosphonium cation allows an antioxidant to accumulate in the mitochondria.

Fig. 2. Effect of MitoTEMPO on mitochondrial H_2O_2 and superoxide in tissue extracts of ischemic skeletal muscle

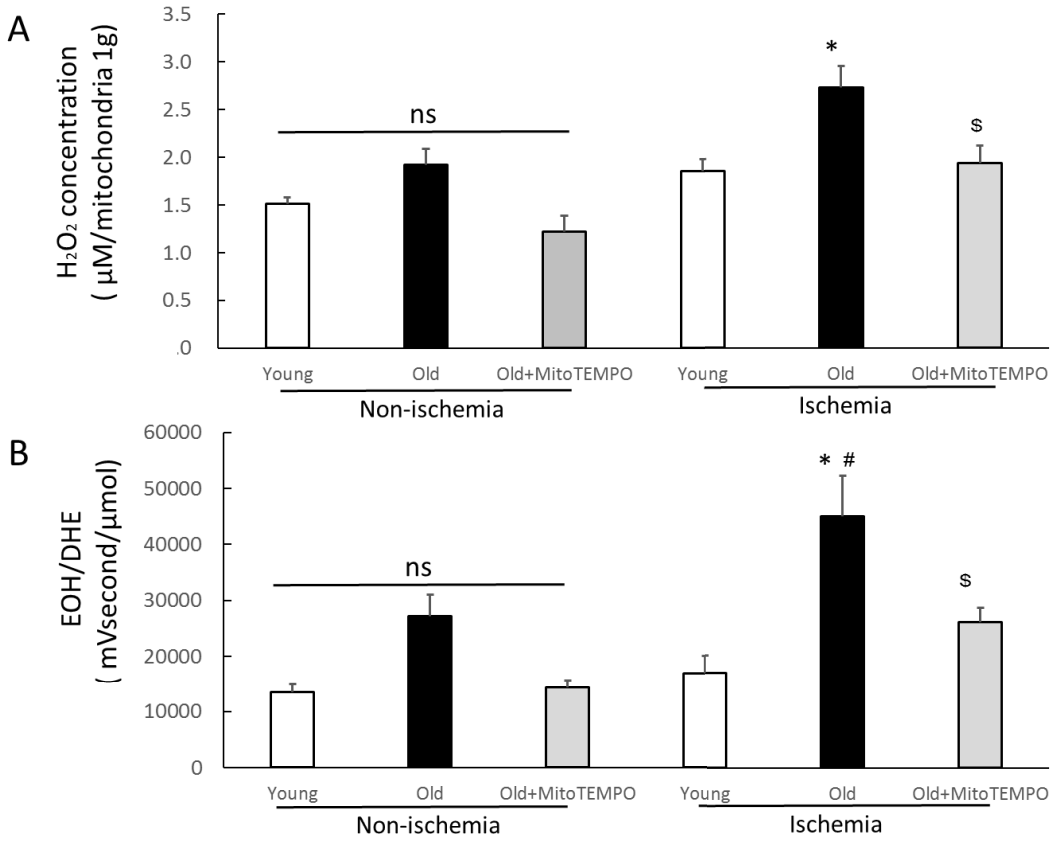

The mitochondrial H_2O_2 concentration was measured in non-ischemic and ischemic (POD 2) skeletal muscle from young, old, and MitoTEMPO-treated old mice (A). The levels of superoxide in tissue extracts were determined by the UPLC method (B). The levels of mitochondrial H_2O_2 and superoxide in tissue extracts under ischemic conditions were higher in old mice than in young mice from the ischemic group. MitoTEMPO treatment decreased the levels of mitochondrial H_2O_2 and superoxide in tissues to levels of young mice. The values are expressed as the means±S.E.M. n=10, each. *P<0.05 vs. young mice, $^{\$}P$<0.05 vs. old mice, $^{\#}$ P<0.05 vs. non-ischemic skeletal muscle.

Fig. 3. Effect of MitoTEMPO on age-related impairment of collateral growth after ischemia

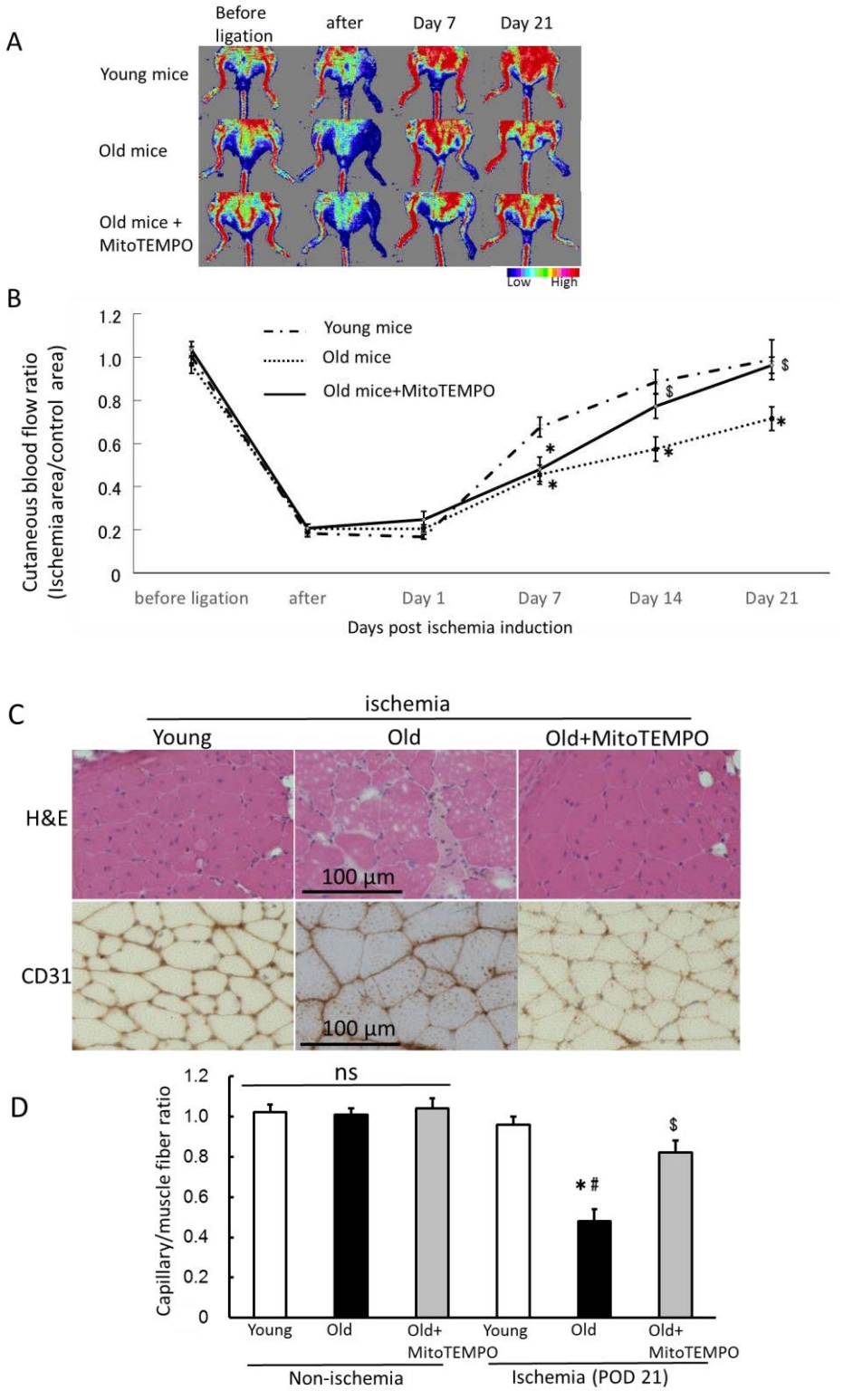

Representative hind limb perfusion imaging after inducing hindlimb ischemia in young, old and MitoTEMPO-treated old mice (A). Ischemic /non-ischemic limb blood flow ratio was used for quantitative analysis (n=10, each. *P<0.05 vs. young mice, $^{\$}P$<0.05 vs. old mice.) (B). Representative sections after H&E staining and immunohistochemical staining. Immunohistochemical staining was performed using anti-CD31 antibody to determine the capillary density of ischemic muscle on POD 21 (C). Quantification of capillary density was shown as the capillary/muscle fiber ratio (n=10, each. *P<0.05 vs. young mice, $^{\$}P$<0.05 vs. old mice, $^{\#}P$<0.001 vs. old mice in non-ischemia.) (D). The values are expressed as the means±S.E.M.

Fig. 4. Effect of MitoTEMPO on mtDNA damage after ischemia induction

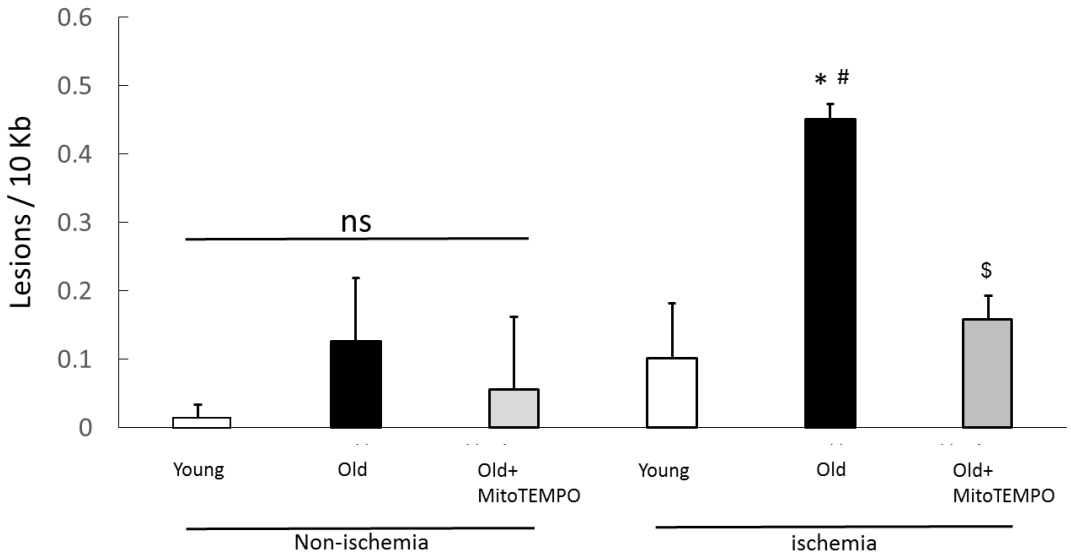

mtDNA damage was increased in old mice compared to young and MitoTEMPO-treated old mice 2 days after ischemia induction, but not in non-ischemic muscles. The values are expressed as the means±S.E.M. n=10, each. **P*<0.05 vs. young mice, $^{\$}P$<0.05 vs. old mice, $^{\#}P$<0.05 vs. non-ischemic muscle.

Fig. 5. Respiration profile from isolated mitochondria in soleus

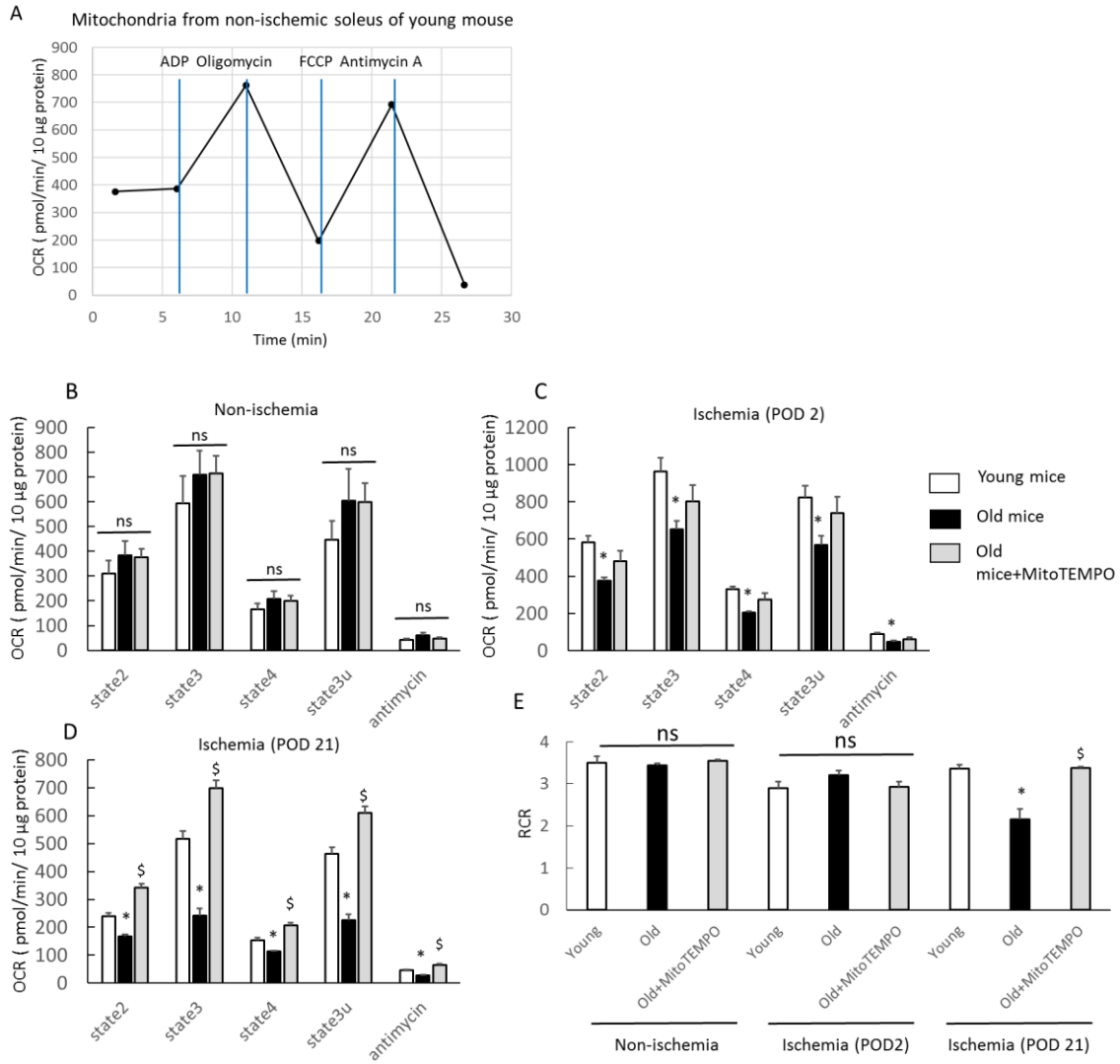

The mitochondrial respiration profile was assessed using the XF24 flux analyzer in non-ischemic and ischemic (POD 2 and 21) skeletal muscles of young, old and MitoTEMPO-treated old mice. A representative figure of XF24 coupling assay using mitochondria from non-ischemic skeletal muscles of young mouse, and OCR response to ADP, oligomycin, FCCP and antimycin A (A). States 2, 3, 4, and 3u respiration and response to antimycin in non-ischemic skeletal muscles did not differ among the three groups (B). States 2, 3, 4, and 3u respiration and response to antimycin in ischemic

skeletal muscles (POD 2) were lower in old mice than that in young mice. MitoTEMPO treatment did not affect mitochondrial respiration (C). States 2, 3, 4, and 3u respiration and response to antimycin in ischemic soleus (POD 21) were lower in old mice than that of young mice. MitoTEMPO treatment preserved mitochondrial respiration (D). The respiratory control ratio (RCR: state 3/state 4 respiration in the presence of succinate) of ischemic soleus (POD 21) was lower in old mice than in young and MitoTEMPO-treated old mice, whereas that of non-ischemic and ischemic (POD 2) skeletal muscles did not differ among the three groups (E). The values are expressed as the means±S.E.M. n=10, each. **P*<0.05 vs. young mice, $^{\$}P$<0.05 vs. old mice. ns indicates no significant difference.

Fig. 6. The protein expression of HIF-1α and VEGF

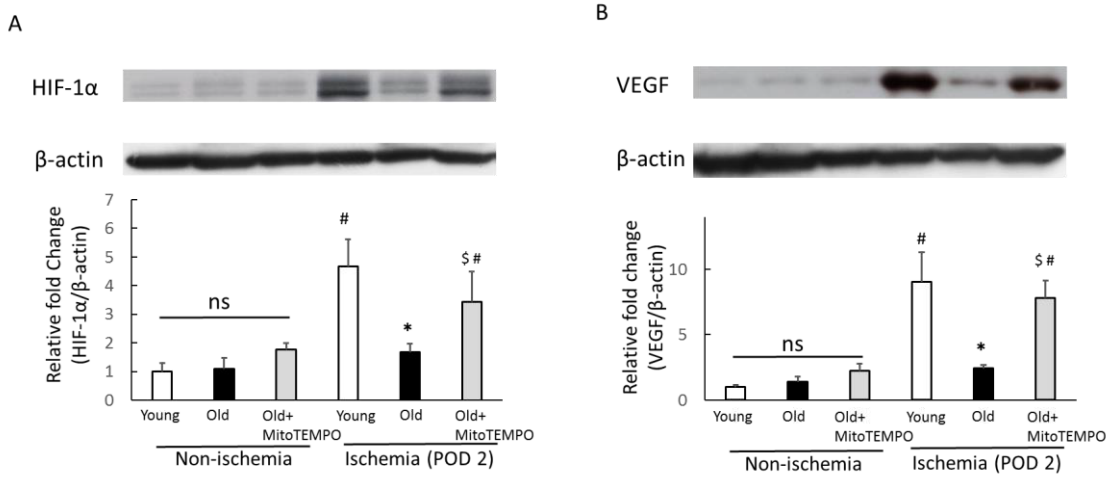

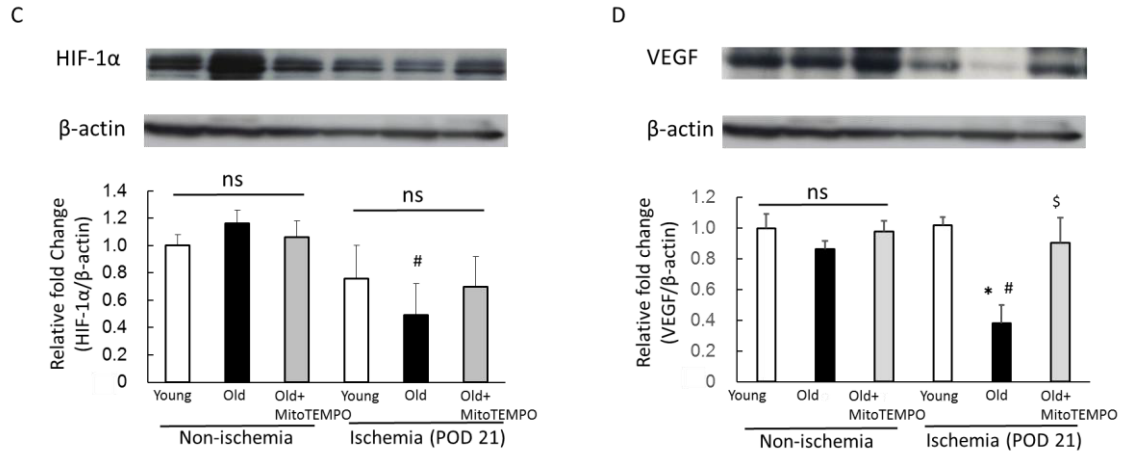

The protein expression of HIF-1α and VEGF were analyzed by western blotting in the non-ischemic and ischemic (POD 2 and 21) skeletal muscles of young, old and MitoTEMPO-treated old mice. Representative images of HIF-1α (A, C: POD 2, 21, respectively) and VEGF (B, D: POD 2, 21, respectively) and summarized findings after quantification of HIF-1α/β-actin and VEGF/β-actin. For POD 2, both HIF-1α and VEGF expression during ischemia were higher in young mice than in non-ischemic mice, but not in old mice. MitoTEMPO treatment upregulated HIF-1α and VEGF expression in the skeletal muscle of old mice. For POD 21, neither HIF-1α nor VEGF expression under ischemia were elevated compared to non-ischemic mice. HIF-1α expression did not differ among the three groups. The VEGF expression of aged skeletal muscle was lower than young muscle, and MitoTEMPO treatment preserved the expression of VEGF. The values are expressed as the means±S.E.M. n=10, each. *P<0.05 vs. young mice, $^{\$}P$<0.05 vs. old mice, $^{\#}P$<0.05 vs. non-ischemic skeletal muscle. ns indicates no significant difference.

Fig. 7. The protein expression of p53

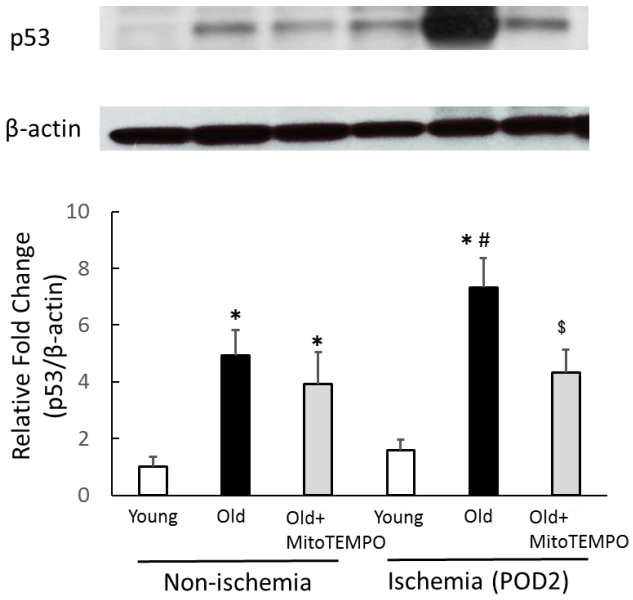

The protein expression of p53 was analyzed by western blotting in non-ischemic and ischemic (POD 2) skeletal muscle from young, old and MitoTEMPO-treated old mice. Representative images of p53 (A) and the summarized findings after quantification of p53/β-actin (B). p53 expression was higher in old mice compared to young mice for non-ischemic and ischemic (POD 2) skeletal muscles. MitoTEMPO treatment attenuated the elevation of p53 after induction of ischemia. The values are expressed as the means±S.E.M. n=10, each. *P<0.05 vs. young mice, $^{\$}P$<0.05 vs. old mice, $^{\#}P$<0.05 vs. non-ischemic skeletal muscle. ns indicates no significant difference.

Fig. 8. The protein expression of PGC-1α, NRF-1 and ERRα

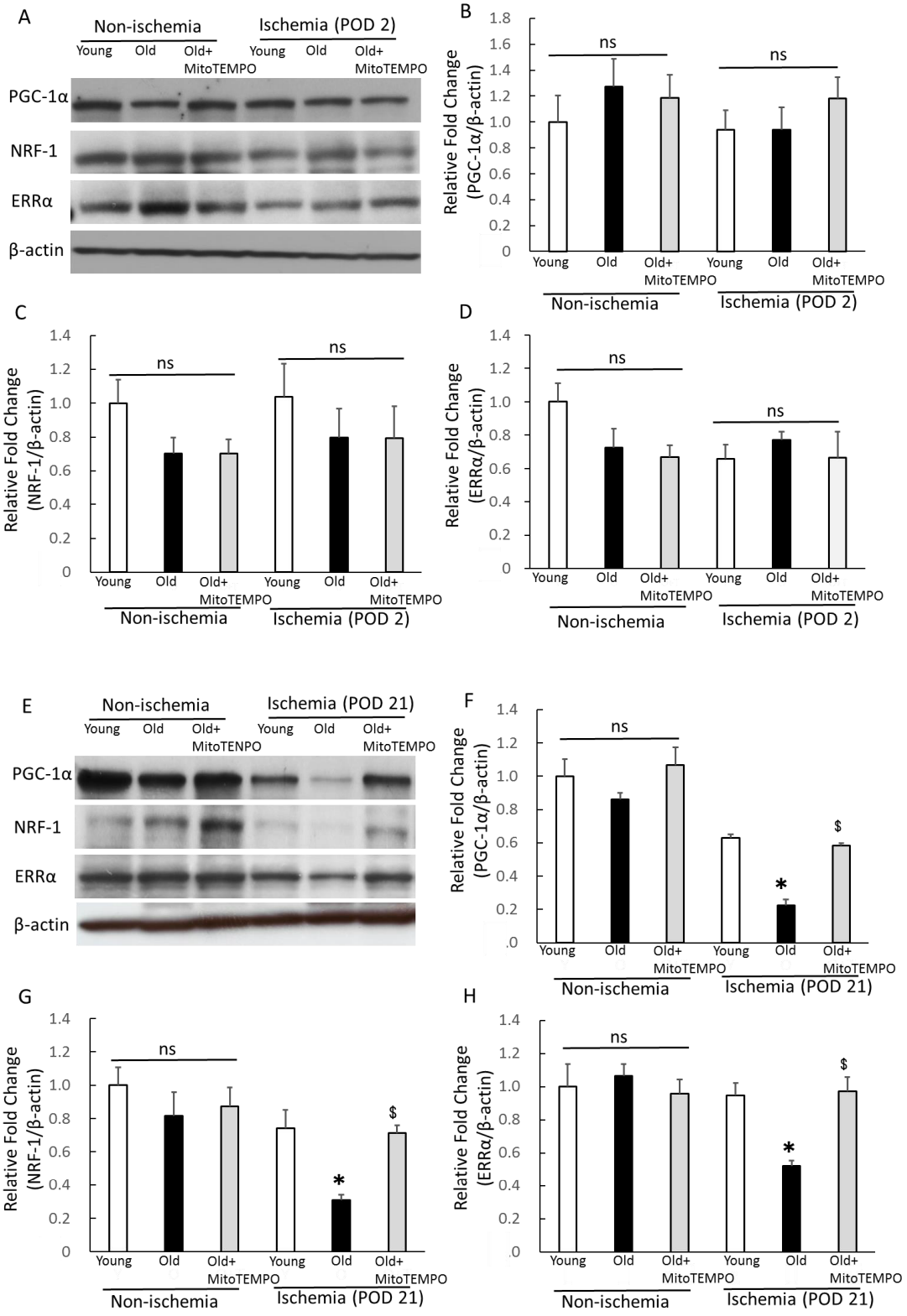

Protein expression of PGC-1α, NRF-1 and ERRα was analyzed by western blotting in the non-ischemic and ischemic (POD 2 and 21) skeletal muscles of young, old and MitoTEMPO-treated old mice. Representative images of PGC-1α, NRF-1 and ERRα for POD 2 (A) and POD 21(E) and the summarized findings after quantification of PGC-1α/β-actin (B, F: POD 2, 21, respectively), NRF-1/β-actin (C, G: POD 2, 21, respectively) and ERRα/β-actin (D, H: POD 2, 21, respectively). For POD 2, the expression of PGC-1α, NRF-1 and ERRα did not differ among the three groups. For POD 21, the expression of PGC-1α, NRF-1 and ERRα was lower in old mice than young mice. MitoTEMPO treatment effectively preserved PGC-1α, NRF-1 and ERRα expression to similar levels as young mice. The values are expressed as the means±S.E.M. n=10, each. *P<0.05 vs. young mice, $^{\$}P$<0.05 vs. old mice. ns indicates no significant difference.

Fig. 9. The protein expression of Bax and Bcl2

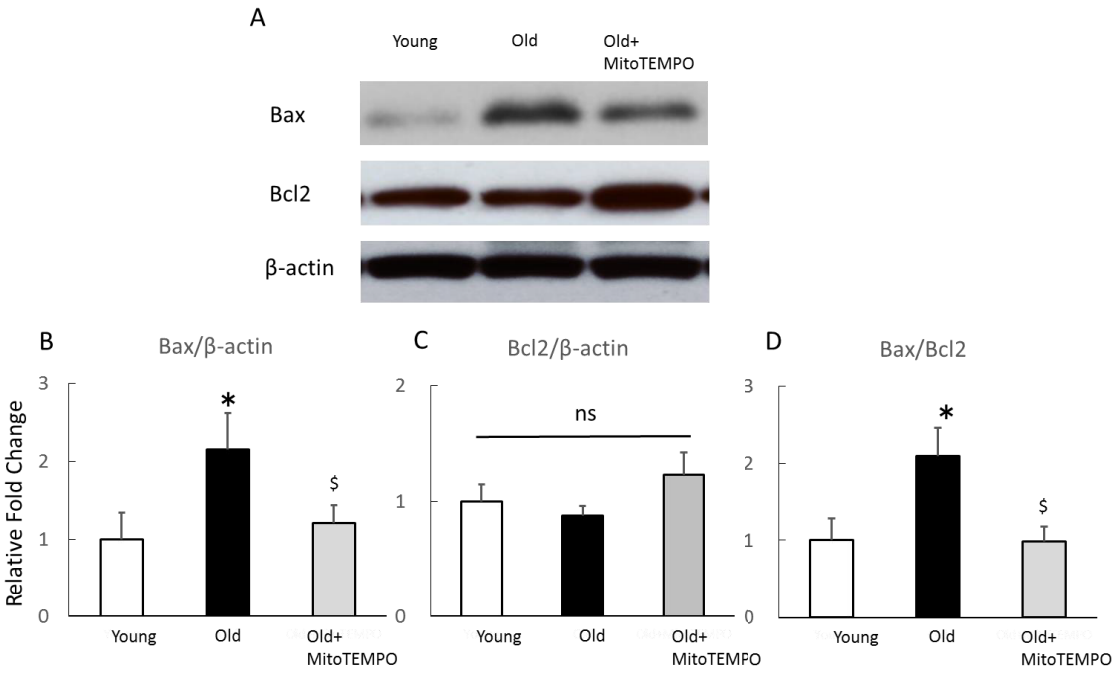

Protein expression of the proapoptotic factor Bax and the antiapoptotic factor Bcl2 was analyzed by western blotting in the ischemic (POD 2) skeletal muscles of young, old and MitoTEMPO-treated old mice. Representative images of Bax and Bcl2 (A) and the summarized findings after quantification of Bax/β-actin (B), Bcl2/β-actin (C) and Bax/Bcl2 (D). The Bax/Bcl2 ratio was significantly higher in old mice compared to young mice. MitoTEMPO treatment decreased the Bax/Bcl2 ratio to a similar level to that of young mice. The values are expressed as the means±S.E.M. n=10, each. **P*<0.05 vs. young mice, $^{\$}$*P*<0.05 vs. old mice. ns indicates no significant difference.

Fig. 10. The role of mitochondrial ROS in the regulation of collateral development with ischemia in aging

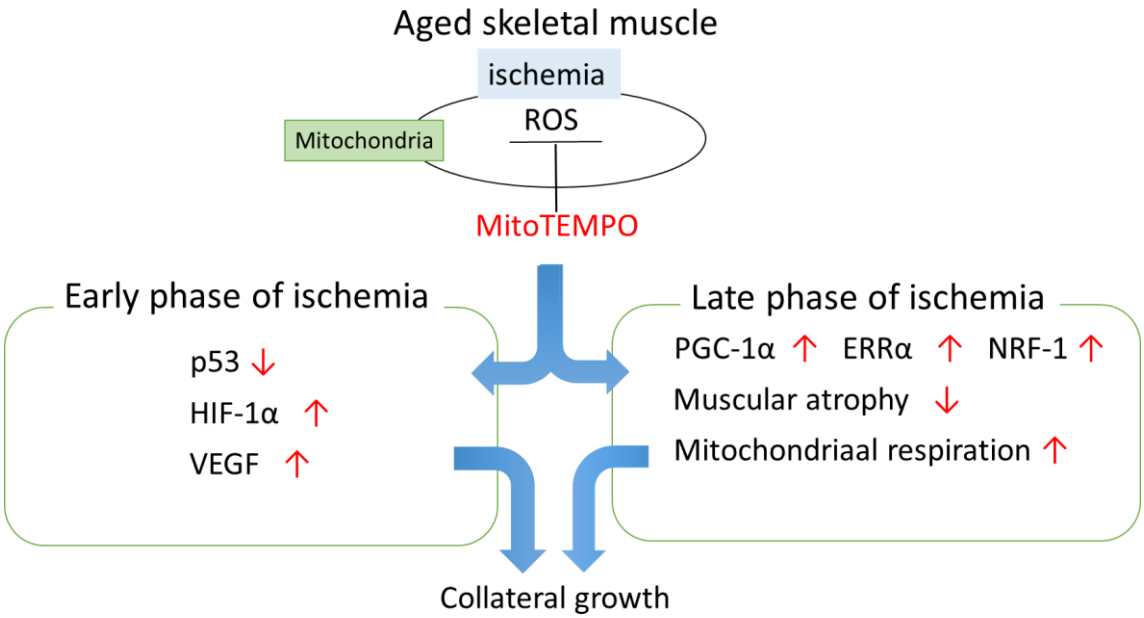

In aged muscle, mitochondrial ROS induced by ischemia impairs collateral development. Mitochondrial ROS scavenging improves collateral growth related to downregulation of p53, upregulation of HIF-1α and VEGF in the early phase of ischemia, and preservation of PGC-1α, NRF-1, and ERRα in the late phase of ischemia. Scavenging of mitochondrial ROS with MitoTEMPO is an effective means to preserve collateral development.

Table. Body weight of mice and weight of hind limb, gastrocnemius-soleus muscle

The ratio of ischemic hind limb (POD 21) to non-ischemic hind limb and the ratio of ischemic gastrocnemius-soleus muscle (POD 21) to non-ischemic gastrocnemius-soleus muscle were lower in old mice than young and MitoTEMPO-treated old mice. The values are expressed as the means±S.E.M. n=10, each. *P<0.05 vs. young mice, $^{\$}P$<0.05 vs. old mice.

		Young mice	Old mice	MitoTEMPO-treated old mice
B.W. (g)		19.6±0.2	28.2±0.2*	28.7±0.3*
hind limb (mg)	ischemia	955.0±21.4	887.8±33.5	1047.2±31.0
	Non-ischemia	1096.3±9.9	1230.5±23.7	1264.4±47.5
	Ischemia/non-ischemia	0.87±0.01	0.72±0.02*	0.83±0.02 $^{\$}$
Gastrocnemius-soleus muscle (mg)	ischemia	62.7±5.6	69.4±2.8	87.5±8.6
	Non-ischemia	75.4±4.0	118.3±2.0	115.1±5.4
	Ischemia/non-ischemia	0.82±0.03	0.58±0.02*	0.75±0.04 $^{\$}$